Immobilising oils in geopolymer cements using Pickering emulsions

Jessica B. McWilliams[1], Hajime Kinoshita[1], Brant Walkley[1], John L. Provis[1,2*]

[1] *School of Chemical, Materials and Biological Engineering, University of Sheffield, Sheffield S1 3JD, UK*

[2] *PSI Center for Nuclear Engineering and Sciences, Paul Scherrer Institut, Forschungsstrasse 111, 5232 Villigen PSI, Switzerland*

**corresponding author, email john.provis@psi.ch*

Abstract

Silica fume was investigated as a potential Pickering agent as an alternative route of immobilisation of organic oils (Nevastane oil or TPB/dodecane) in potassium geopolymer cement. The Pickering emulsion was able to immobilise up to 30 wt% Nevastane loading in the geopolymer cement. The formation of the Pickering emulsion was able to decrease the initial and final setting times, whilst, increasing the early compressive strength of the Pickering samples in comparison to non-emulsified Nevastane samples. The X-ray tomography data further showed the successful dispersion of the Nevastane droplets throughout the geopolymer matrix, with good uniformity of the droplet distribution. However, the Pickering emulsion was unable to successfully immobilise the TBP/dodecane at any weight loading, suggesting that this immobilisation route was not suitable for this particular organic oil. Hence, Pickering emulsions could be used as an alternative route for the immobilisation of selected organic oils into geopolymer cements.

Keywords: Geopolymer, nuclear waste immobilisation, oil, cement, Pickering emulsion

1. Introduction

Cement has been widely used for nuclear waste immobilisation, particularly for low level and intermediate level wastes, because it is a versatile, cheap, easy process, and the resulting wasteform has high radiation stability, and is fire and impact resistant [1]. However, cementation increases the volume of the waste, and Portland cement may be sub-optimal for incorporating organic liquid waste; addition of various types of organics at high loadings will result in strong retardation meaning that the cement will not set effectively [2]. Adding an organic liquid that is immiscible with water makes the system more complicated because it has two individual liquid phases and a large quantity of solid particles [2]. Geopolymers, a type of alkali-aluminosilicate alternative cement, have been suggested as a potentially viable alternative as they undergo a polycondensation reaction which is relatively unaffected by the addition of organic liquids, and so are able to set despite incorporation of these wastes at high loadings [3].

The organic liquids which are the focus of this research are a lubricant oil, and a mixture of tributyl phosphate (TBP) with dodecane. Oils are used as lubricants in nuclear fuel cycle processing and manufacturing equipment, and become classified as secondary nuclear waste due to radiological contamination. The TBP/dodecane (or kerosene) blend is used in the nuclear sector during the PUREX (plutonium uranium redox extraction) process to extract valuable elements from spent nuclear fuel to be reused [4]. During the PUREX process, the spent mixture of TBP/dodecane or kerosene is irradiated and forms radiolysis products - the majority of which is dibutyl phosphate (DBP), monobutyl phosphate (MBP), organic acids and butanol. Radioactive waste loadings of 300 μg/mL of uranium, thorium, plutonium, and other radionuclides release alpha radioactivity that has been measured at levels as high as 9.67 Bq/mL [4]. This contamination and the liquid nature of the spent organic extractant from the PUREX process means that it needs to be conditioned into a solid form for eventual disposal. Nevastane EP100 oil is a generic lubricant oil used to represent the general oil waste produced from the nuclear industry. TBP/dodecane and Nevastane EP100 are both classified as problematic wastes as there is currently no defined route for disposal.

Organic wastes such as oils can be immobilised in cement by three different techniques: direct incorporation, pre-emulsification, and solid impregnation; Figure 1 [5]. Direct incorporation involves directly adding the organic oil into the cement slurry. Pre-emulsification requires the formation of a stable emulsion (either by the addition of surfactants or Pickering agents), before the addition of the cement precursor. Solid impregnation requires the organic oil to be absorbed into a solid precursor which is then added to the aqueous component [5].

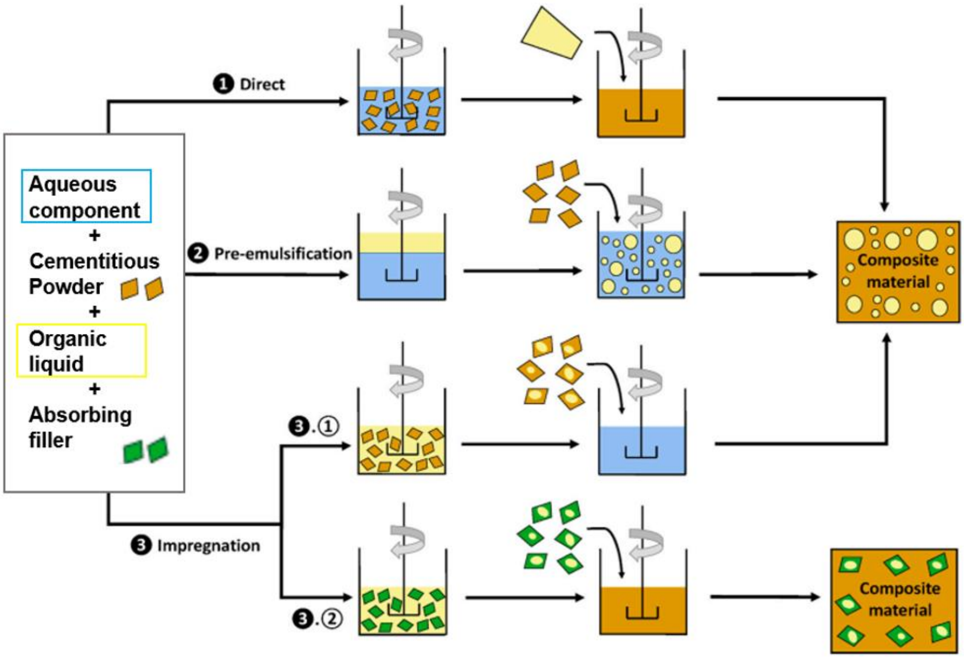

Figure 1 – The three pathways for oil to be incorporated to either AAMs or Portland cement, adapted from Reeb *et al.* [5]

Lambertin *et al.* [6] researched and patented geopolymers which could direct incorporate 20 to 70% organic liquid (based on the composite material volume) with 1 - 10% of surfactant. TBP was among the list of organic liquids that could be directly incorporated. However, their patent states that direct immobilisation into the geopolymer should not lead to any leaching if the final material has no structural defects [6]. Pierlot *et al.* [7] found, for metakaolin geopolymers, that incorporation rates for oils greater than 10 %vol or with a viscosity lower than 1.0 Pa·s. there is a tendency toward oil coalescence and resulting separation of the oil.

Cantarel *et al.* [8] also researched geopolymer assembly by emulsion templating to stabilise various organic liquids up to 70 vol%. This paper reported production of geopolymers with different surfactants (L35 and CTAB) to highlight the influence of surfactants in the immobilisation of hexadecane. When the surfactants were not added, the hexadecane had the quickest phase separation. With the surfactants, it produced flocculation, so their presence caused a high resistance against coalescence. Work by Bertin *et al.* [9] found that CTAB was able to allow stability of a water/dodecane system via Pickering effects; a Pickering emulsion is when very small solid particles build up at the interface of two immiscible liquids and act as stabilisers [9]. However, the CTAB would partially precipitate out of the emulsion, making it an unsuitable surfactant for this work [10].

Impregnation of metakaolin geopolymers with 8 vol% organic liquid of Cu^{2+} with LIX-84 (2-hydroxy-5-nonyl acetophenone) was carried out by El-Nagger *et al.* [11] The leaching tests (confirmed by FTIR) found that most of the Cu^{2+} and solvent had not travelled out of the cement. The compressive strength was found to be less than 4 MPa, so was too low for many applications, but the leaching rate here was favourable. In total 5% of the Cu^{2+} was leached; the lack of leaching is likely due to the Cu^{2+} being immobilised [11]. Mossini *et al.* [12] investigated using the pre-impregnation route to immobilise 10 and 20 wt% of TBP/Kerosene (30/70) with NOCHAR polymer. The NOCHAR N910 elastomeric polymer was found to be more stable in the alkaline environment with 5 wt% used as an absorbing material for 10 wt% TBP/Kerosene as there was no leaching during the mixing or setting of the samples [12]. However, the compressive strength was still reduced to 5.9 MPa after 28 days of curing, which is below the industry standard [12].

When organic oils are added to the geopolymer matrix via blending with the aqueous alkaline activator, this may lead to formation of an unstable emulsion of oil in the potassium silicate activating solution. This instability will then result in the separation of the liquid and the oil [13]. To retain stability, as required for formation of a more uniform distribution of the encapsulated oil within the conditioned wasteform, emulsifying agents are required. Emulsifying agents would conventionally be surfactants (ionic or non-ionic), but it is also possible to use very fine solid particles (either inorganic or organic) to create a Pickering emulsion [13]. The use of surfactants has to be carefully monitored as they can cause damage to the environment if released [14], and their interactions with waste radionuclides may be complex and may result in more rapid leaching of immobilised species. Therefore, this work will investigate the use of Pickering emulsions as a potential alternative route for the immobilisation of liquid organic oils in geopolymer cement.

A Pickering emulsion works by creating a layer of solid particles between the liquid and the oil, to minimise interfacial tension and cause the emulsion to have greater stability; Figure 2 [13]. The solid particles attach to the interface and can provide enhanced stability due to strong absorption at the oil-water interface and the formation of a rigid mechanical barrier [15]. This reduces the likelihood of Pickering coalescence occurring. Pickering coalescence is the process where the droplets in the Pickering emulsion combine together to create a larger droplet.

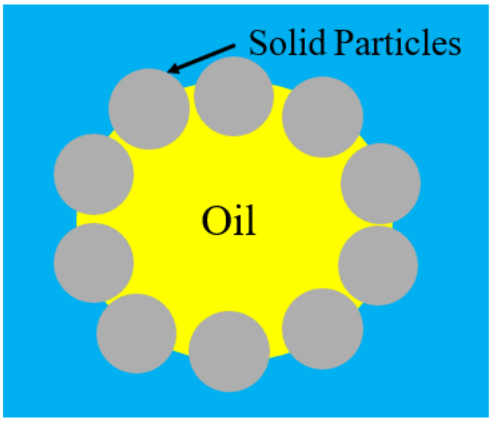

Figure 2 – A diagram of how a Pickering emulsion is formed with hydrophobic solid silica particles embedded in the oil droplet

Silica fume is a very fine (nanosized), amorphous form of silicon dioxide and is a by-product in the production of silicon and ferrosilicon alloys in electric arc furnaces [13], which has been widely used in the construction industry for increasing the strength of concrete [16]. It can improve the packing density of a cementitious binder by its ultrafine particles filling in the matrix, and also reacts as an alkali-reactive and pozzolanic material. Silica fume and fumed silica (which is a manufactured product of similar particle dimensions) have both been investigated for their Pickering emulsification properties. For example, Levine *et al.* [17] were able to stabilise an O/W emulsion (toluene/water) by using hydrophilic silica nanoparticles (572 nm in diameter) which formed a monolayer at the O/W interface.

Griffith & Daigle [18] further investigated the effect of hydrophilic and hydrophobic silica fume in terms of destabilisation of Pickering emulsions, and concluded that the ability to coalesce the emulsion is related to the wettability of the silica fume by the continuous phase. The same authors [18] also highlighted that using hydrophobic silica fume would be detrimental to the stability of the Pickering emulsion as it would destabilize it. Instead, it would be beneficial to use hydrophilic silica fume as it retains the stability of the Pickering emulsion.

Frelichowsha *et al.* [19] investigated creating Pickering emulsions with various oils at 20 wt%, using 6 wt% bare silica. The hydrophilic fumed silica was able to form successful emulsions with polar oils such as butanol, ethyl acetate and butyl lactate. The oil droplets were dispersed as a milky emulsion. The unsuccessful emulsions involved non-polar oils such as mineral oil, silicon oil and diethyl hexyl adipate. This was because the oil had a lower density than the other liquid so rose to the top, joining together to create a cream layer; this process is known as creaming. This work concluded that the favourable oils to form a Pickering emulsion were more polar and short-chained e.g. mono or diesters [19].

Another advantage of incorporating silica into the geopolymer matrix is shown in work by Zhang *et al.* [20] where the addition of < 1.0 % nano-SiO_2 particles was able to increase the fluidity of the geopolymer matrix. This was due to the silica being able to full any voids in the matrix and increased the lubrication. At > 1.5 % nano-SiO_2 particles, there was absorption of free water due to the large specific surface area, decreasing flowability of the geopolymer [20]. Lo *et al.* [21] found that addition of 0.5 wt% nano-SiO_2 particles, increased the compressive strength as the silica was able to fill any voids in the geopolymer matrix. Zawrah *et al.* [22] also found that there was an optimum silica incorporation of 2.5 %. Above 2.5 % nanosilica, the compressive strength decreased due to the nano-SiO_2 particles aiding in the breakdown of the geopolymer gel. The work of Zhang *et al.*, Lo *et al.* and Zawrah *et al.* is important as background for the current study, as the addition of silica to geopolymer could have additional value apart from creating a Pickering emulsion [20-22], as filling of voids or cracks in the geopolymer matrix would be beneficial for geopolymer samples containing oils as it would mitigate the additional porosity caused by the presence of the oils. This would require the addition of extra silica to the geopolymer matrix to act in this way without compromising the emulsion stability. However, if the quantity of the nano-silica is too high, it would be expected to have negative effects on the geopolymer gel and, hence, impact mechanical properties such as compressive strength.

In conclusion, the literature shows that organic oils can be immobilised by three routes – direct incorporation, pre-emulsification and impregnation [5]. However, neither of these routes has been found to be robustly successful in immobilising TBP/dodecane or Nevastane EP100 into geopolymer cement for nuclear waste storage. Pre-emulsification with Pickering agents is an alternative immobilisation route that has not been explored extensively in the literature. The literature shows that Pickering emulsions can be successfully created by using silica particles. This work will focus on creating Pickering emulsion with hydrophilic silica particles to incorporate high loadings of organic oils into geopolymer matrices, with the aim of developing a viable matrix for the encapsulation of liquid radioactive organic wastes resulting from operations and processes in the nuclear fuel cycle.

2. Experimental

This work investigates the creation of Pickering emulsions with silica fume (dosed at 1 wt.% relative to the mass of the organic oil) used to emulsify TBP/dodecane (30/70, where dodecane represents the industrially-used kerosene in the PUREX process) and Nevastane EP100 oil (mixture based on white mineral oil, synthetic oils and high-performance additives), which are incorporated at 10, 20, 30 and 40 wt.% loadings into geopolymer formulations that have been developed by the UK National Nuclear Laboratory for the PREDIS European Project, Table 1 [23]. The 1 wt.% of silica fume (particle size ~ 5 – 50 μm as-supplied, consisting of loose aggregates with primary particles 0.01 – 0.2

μm in size) relative to the quantity of organic oil was chosen due to the findings in the literature where 0.5 – 2.5 wt.% (relative to the oil) of silica to create a Pickering emulsion was found to have the optimum properties [20-22]. In forming a Pickering emulsion, the aggregated silica fume is expected to disperse and release the primary particles to act individually.

The geopolymer formulation is defined by the SiO_2/K_2O and H_2O/K_2O molar ratios of the activating solution (prepared using commercial products from Sigma Aldrich), and the bulk K_2O/Al_2O_3 molar ratio of the mix (which thus defines the proportions between the activator and metakaolin constituents). The metakaolin used was Metamax (BASF), mean particle diameter of 1.2 μm and SiO_2/Al_2O_3 ratio of 1.2; Table 2.

Table 1 – The baseline geopolymer formulation tested in this work, defined in terms of molar ratios

Metakaolin	**Activator SiO_2/K_2O**	**Activator H_2O/K_2O**	**Bulk K_2O/Al_2O**
Metamax	1.2	13	1.2

Table 2 – The chemical composition, in wt%, of Metamax metakaolin obtained by X-ray fluorescence (XRF). LOI is loss on ignition [24]

Compound	**Metamax**
SiO_2	52.5
Al_2O_3	44.5
TiO_2	1.3
Fe_2O_3	0.4
CaO	Trace
K_2O	0.2
Na_2O	0.2
LOI	0.6
Others	0.2

The silica particles, alkali activating solution and organic oil, combined in the ratios defined in Table, 3 were mixed for five minutes at 2000 rpm – this allowed time for the Pickering emulsion to form. Afterwards, the metakaolin was added and mixed for five minutes at 2000 rpm to allow the formation of the geopolymer gel. The mixing was then paused so that any residual materials on the sides of the bowl can be removed and added back into the bulk of the material. The mixing was then continued for a final five minutes, and the paste then transferred to a suitable mould for curing and later analysis. The samples were cured at 20 ºC in relative humidity at for set time period i.e. seven, 28 and 90 days.

Direct immobilisation of the organic oils was used as a baseline to understand the effect the Pickering emulsion was having on the immobilisation of the organic oils in the geopolymer matrix. In direct immobilisation, the organic oil is mixed directly with alkali activating solution and metakaolin for 10 minutes at 2,000 rpm. This method does not use silica fume to create a Pickering emulsion, or any surfactants for formation of emulsions to aid in the incorporation of the organic oils.

Table 3 – The percentage by weight of each oil in the geopolymer formulation, where the binder composition as defined in Table 1 was molar ratios 1.2/13/1.2 of K_2O/Al_2O_3, H_2O/K_2O and SiO_2/K_2O

Sample	**Oil**	**Oil loading (wt% relative to geopolymer)**	**Silica particles (wt.% relative to geopolymer)[a]**
KGp	None	-	-
A1	TBP/dodecane	10	0, 0.1
A2	TBP/dodecane	20	0, 0.2
A3	TBP/dodecane	30	0, 0.3
A4	TBP/dodecane	40	0, 0.4
B1	Nevastane	10	0, 0.1
B2	Nevastane	20	0, 0.2
B3	Nevastane	30	0, 0.3
B4	Nevastane	40	0, 0.4

[a] Samples with 0% added silica fume are denoted “Direct” encapsulation; samples containing silica fume (at 1% of the oil loading in each case) are denoted “Pickering”.

Zeta potential measurement was used to understand the stability of the Pickering emulsion as a function of pH; rheology, compressive strength and Vicat setting time testing were carried out to investigate the workability, strength and initial/final setting times of the various geopolymer matrixes; respectively. Details of all tests are given below. If a sample had visible liquid separation, then it was not used for the further analysis of compressive strength, rheology and Vicat setting time. The observed visible separation was reviewed during the initial mixing and pouring into the vials, and after seven days of curing. Fourier transform infrared (FTIR) spectroscopy and X-ray diffraction (XRD) were used to investigate the chemical bonds and crystalline phases in the formed geopolymer matrix; respectively. X-ray tomography was used to create 3D images of the geopolymer matrix to understand how the Pickering emulsion influences the oil distribution. If there was liquid separation, then the segregated layer was removed before FTIR, XRD and X-ray tomographic analysis.

A Stabino Nanoflex instrument with an oscillating piston (diameter 8 mm) was used to measure the zeta potential. The silica particles, Nevastane oil and metakaolin were first investigated separately.

TBP/Dodecane was not measured for safety reasons, because the instrument was not able to be used in a fume hood. Either the silica particles, Nevastane oil or metakaolin, in a ratio of 1 to 100 (0.05/50 g) with deionised water was measured for its zeta potential. Afterwards, the zeta potential was also measured in an alkaline environment (KOH solution) at pH values between 11 and 14.5. The silica/oil/metakaolin was added to the alkaline solution just before the measurements, to avoid the alkaline environment potentially hydrolysing or dissolving the materials. To investigate the stability of the Pickering emulsion, the oil and metakaolin/silica particles were combined at 1/200 (0.025 g) each in deionised water adjusted to the specified pH with KOH, for each pH environment.

The rheometer, in vane geometry, used for the rheology measurements was a Haake Viscotester VT550 (ThermoFisher) with FL100 measuring geometry with a 1.000 mm gap in the blade. The yield stress program was set for 120 seconds with a stepwise clockwise rotation at 0.010 s^{-1}. The plastic viscosity is measured using a three-step program: the shear rate is linearly ramped up for 60 seconds from 1 – 100 s^{-1}. This shear rate is then held for two seconds, and then linearly deceased for 60 seconds, from 100 – 0.0001 s^{-1}. The rheological tests were conducted on fresh pastes immediately after the mixing procedure.

For compressive strength testing, a modified form of the ASTM standard C1928 for alkali-activated mortar compressive strength was used, adjusted to use paste rather than mortar samples [25]. The samples were cured at room temperature, and tested in triplicate.

For Vicat setting times, the BS EN 196-3:2016 method [26] was adapted as needed. This standard requires the material to be mixed for 90 seconds, stopped to remove the samples from the sides for 30 seconds and then mixed again for 90 seconds. However, the addition of oil to the geopolymer material requires more time for the oil to be properly incorporated. Therefore, the mixing was carried out for ten minutes. The sample was then poured into a cylindrical container which is 40 ± 0.2 mm deep and has an internal diameter of 75 ± 10 mm, for testing using a Humboldt automatic Vicat tester. The initial setting time is defined to be when the gap between the needle and the base of the cylinder is between 3-9 mm, and the final setting time is when the needle is only able to penetrate 0.5 mm into the sample. The ATSM C191 standard criteria are used to evaluate the results; the initial and final setting times are considered to be acceptable if they are within the range of 30 to 120 minutes and not longer than 6.5 hours, for the initial and final set; respectively [27].

For the FTIR measurements, a Nicolet iS5 spectrometer was used, in transmission mode at 16 cm^{-1} with a scan time of 64 seconds in the range of 500 - 4000 cm^{-1}. XRD measurements were conducted using a Panalytical X'Pert instrument with a 2θ range of 5-70° 2θ, CuKα radiation (1.54 Å) with a nickel filter, 0.020° step size, and a 2 s/step counting time. In the diffracted beam, an 2.5° Soller slit was used, and an anti-scatter blade was applied to minimise the diffracted background intensity at low angles, with 1.0 nm incident beam divergence. The phases were identified using the Diffrac. EVA V4.1 software with the ICDD PDF4+ 2015 database.

A Zeiss Xradia 620 Versa XRM instrument was used for X-ray tomography with a one-hour run time. The pixel density used was 1024 pixels with 15 µm pixel size. Therefore, each sample was cast as a cylinder with 15 mm diameter, and approximately 24 mm in length. To analyse the X-ray tomography data, Slicer3D was used to produce 3D models of the oil droplets in the geopolymer matrix, and ImageJ was used to analyse the images produced [28].

3. Results and Discussion

Samples of potassium aluminosilicate geopolymers of the formulation defined in Table 1 were prepared with either 10 – 40 TBP/Dodecane (30/70) or Nevastane oil, with and without silica fume (added at 1 wt% of the respective oil wt% loading), Table 1. From the initial observation of the preparation process, it was observed that at 10 wt% TBP/dodecane, there was a layer of liquid above the cement. This was likely to be oil that had not been incorporated in the geopolymer matrix, and had separated due to the unfavourability of the O/W emulsion. When the loading of TBP/dodecane was increased from 10 wt% to 40 wt%, there was a clear separation of the liquids with a significant quantity of the oil sitting above the cement. This suggests that the silica fume was not successful in aiding the immobilisation of the TBP/dodecane by Pickering emulsion.

For Nevastane, when the weight percentage was increased from 10 to 30 wt%, there was an increase in the viscosity of the sample; detailed rheometric analysis of the geopolymer mixes will be presented in Section 3.2 Rheology. The sample with 30 wt% Nevastane was the most viscous of all the samples made and was difficult to pour (See Section 3.2 Rheology). For 10, 20 and 30 wt% there was no formation of a liquid layer on top of the cement sample, which suggests that there was immobilisation of the oil. At 40 wt% Nevastane, there was a decrease in viscosity and was easier to pour than at 30 wt% Nevastane. It also had a ‘shiny’ surface, which suggests that not all of the oil was incorporated. From these initial observations, the Pickering emulsion approach looks to be suitable for quantities of Nevastane up to 30 wt%.

3.1 Zeta Potential

The zeta potential over a pH range of 9 to 14.5 was measured to understand the stability of the Pickering emulsion; Figure 3. The zeta potential measurements indicate the stability of the Pickering emulsion, as a higher magnitude of the zeta potential relates to higher repulsion between the droplets, hence a more stable emulsion. The zeta potential measured for the silica particles had a lowest magnitude at pH 13.5, with a zeta potential of -2.57 mV. This suggests that with increasing pH the stability of the silica particles in the solution decreases, and they begin to flocculate together (and/or to dissolve during the measurement) at higher pH, resulting in a lower magnitude. The samples containing both silica particles and the oil – i.e. the constituents of the Pickering emulsion - showed a similar trend. Therefore, if this charge is uniformly distributed among the different constituents, the silica particles and the oil would be repelling each other, but it is difficult to determine if this is the case from this measurement alone.

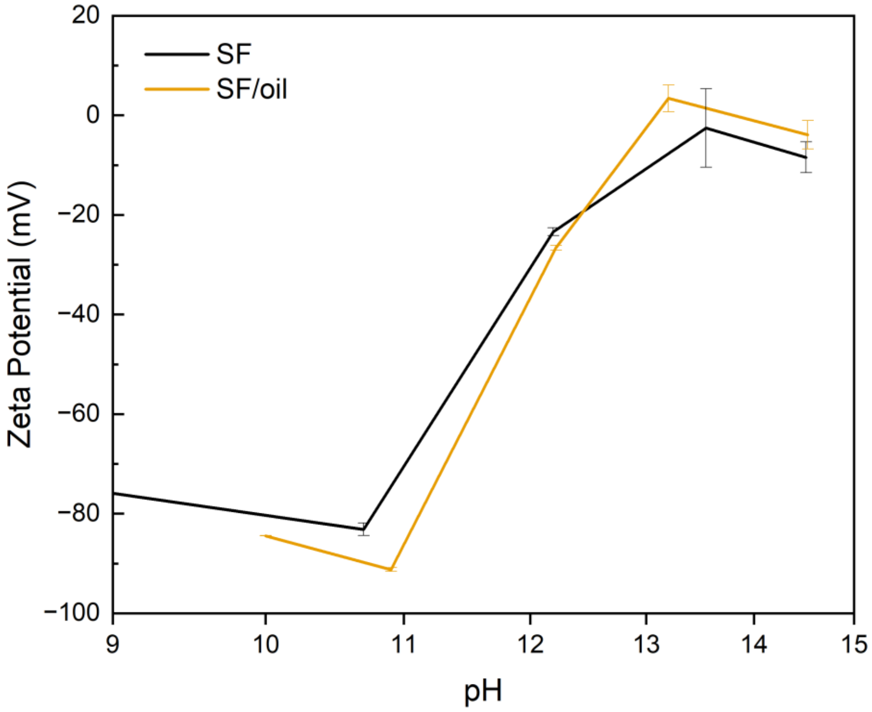

Figure 3 – The measured zeta potential as a function of pH for the silica fume and silica fume/oil systems

When these Pickering samples were compared to the direct incorporation zeta potential measurements, Figure 4, it appears that the addition of the silica particles had little effect on the trend in zeta potential values found with the direct incorporation route. This highlights that the oil, metakaolin and silica particles all have negative charges, so are repelling each other and contributing their negative surface charge to the total zeta potential. If the silica particles contained a positive surface charge, then its positive surface charge would have been attracted to the negative surface charge of either the metakaolin or the Nevastane oil. However, since, the zeta potential does not decrease it can be concluded that the silica particles do not display any positive surface charge.

In the literature, Derkani *et al.* [29] found that metakaolin had an increased negative surface charge when the pH increased from 7 to 12, via deprotonation of the hydroxyl groups of the silicon and aluminium on the metakaolin surface. Silica particles when dissolved in pH 7 also carry a negative charge due to some of the terminal silanol groups dissociating [30, 31]. Sjöberg *et al.* [32] found that during dissolution at pH ≤ 9, silicic acid ($Si(OH)_4$) was formed [32], whilst alkaline environments would result in the formation of monosilicates ($Si(OH)_3^-$, $SiO2(OH)_2^{2-}$) and polysilicates. Therefore, it can be concluded that the silica particles under alkaline conditions have a negative surface charge that aids in the dispersion of the Nevastane oil droplets, reducing the likelihood of oil coalescence and, hence, oil separation from the geopolymer matrix.

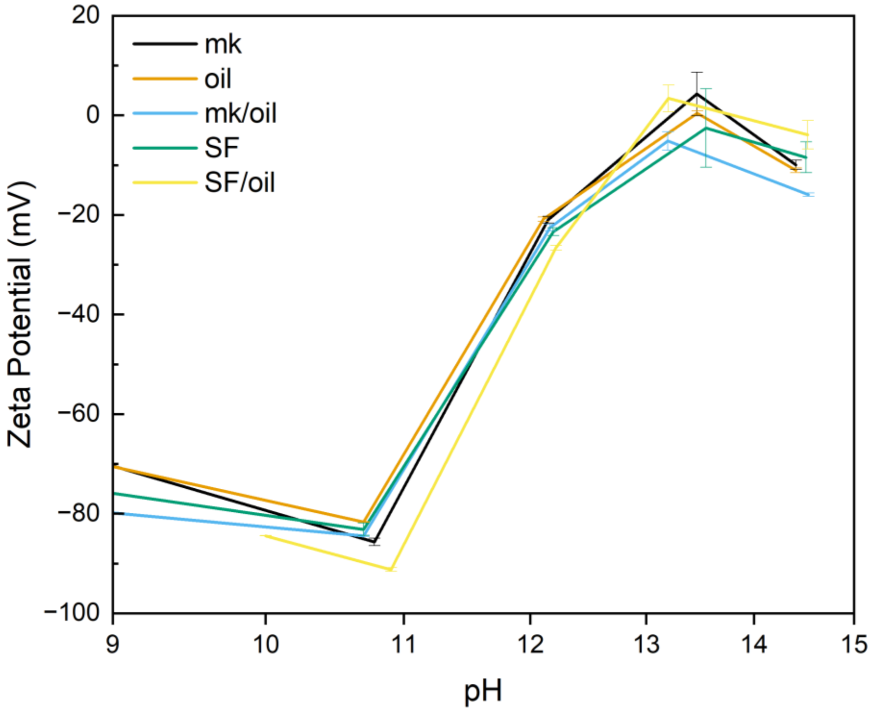

Figure 4 – The average measured zeta potential as a function of pH for samples containing metakaolin, Nevastane oil, metakaolin/Nevastane oil, silica fume, and silica fume/oil systems

When the oil wt% was increased with metakaolin and silica particles, to mimic the Pickering emulsion created in the geopolymer matrix as the oil loading increases, it was found that these samples had a slightly more positive zeta potential value compared to the metakaolin/oil samples as the oil loading increased, Figure 5. The consistent zeta potential measurement of the system with metakaolin, Nevastane oil and silica particles as the oil loading increases suggests that the silica particles are aiding in dispersing the oil more effectively than the direct route. This can be seen at 40 wt% where the direct route has a sudden increase where zeta potential becomes positive, and this is where the oil coalescence is occurring. This oil dispersion occurs at all oil loadings for the Pickering emulsion because the silica particles are also repelling it alongside the metakaolin particles, as evidenced by the X-Ray tomography data in Section 3.7, Figure 14. However, at higher oil loadings such as 40 wt%, this could present an issue, as there are more oil droplets in the geopolymer system. Hence, favourable coalescence could be an issue when the samples are scaled up and the oil droplets could reach a critical limit where they can coalesce from the geopolymer matrix [33].

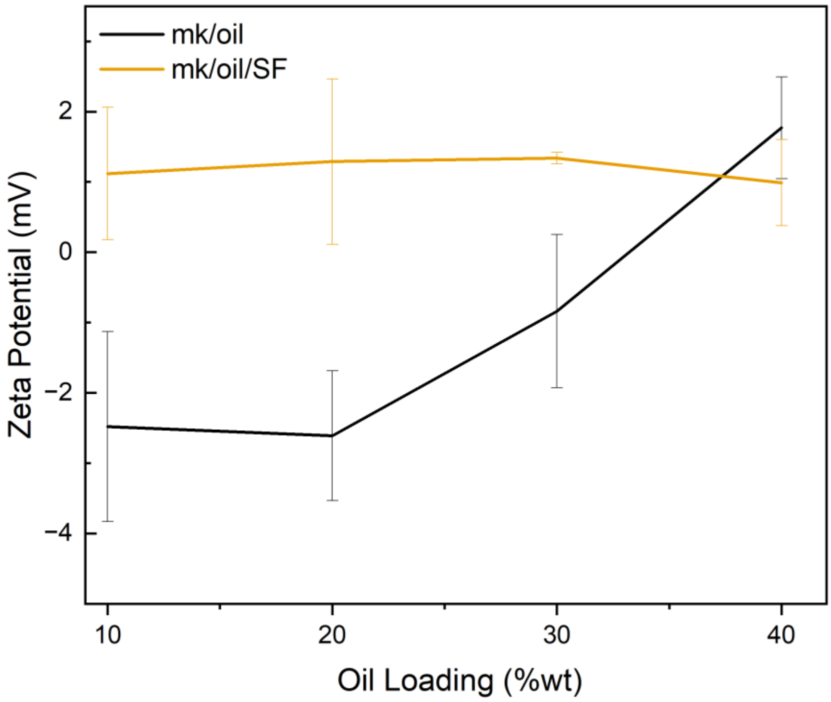

Figure 5 – The average measured zeta potential as a function of the oil loading of Nevastane oil for metakaolin/oil and metakaolin/oil/silica particle systems at pH 14.

3.2 Rheology

The initial flow curves showed as Nevastane oil was added to the geopolymer matrix with 1 wt% silica, the shear stress increased, Figure 5. The 10 wt% Nevastane Pickering sample had a higher resistance to flow than the oil-free sample, while the 20 and 30 wt% Nevastane Pickering samples had an increased shear stress compared to the 10 wt% Pickering samples. Conversely, the shear stress dropped to mirror the rheology of the geopolymer cement with no incorporated Nevastane oil for the 40 wt% Pickering sample; Figure 6. These results mirror the physical observations found during the mixing and pouring of the samples: for the 10 to 30 wt% Nevastane Pickering samples, the samples became more difficult to pour at increased oil loading due to increase viscosity and reduced flowability, while, the 40 wt% Nevastane Pickering sample was easier to pour due to decreased viscosity and increased flowability because of the Nevastane oil separation from the geopolymer matrix.

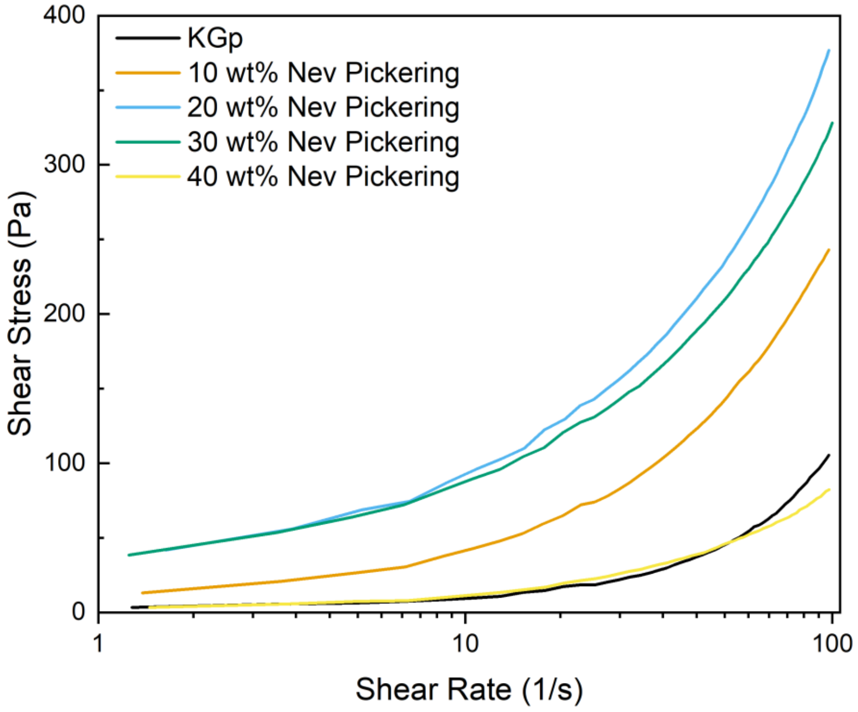

Figure 6 – The flow curves of potassium geopolymer samples as a function of the weight percentage of Nevastane emulsified using silica particles; ascending shear ramp

The Bingham and Herschel-Bulkley models were applied to the curves to understand the flow relationships of the Pickering samples. The Bingham model is used for non-Newtonian fluids and describes their behaviour via two parameters, yield stress and plastic viscosity; Eq 1. The Herschel-Bulkley model is a three-parameter model also used for non-Newtonian fluids; Eq 2.

Eq. 1

$$\tau = \tau_0 + K\dot{\gamma}$$

Eq. 2

$$\tau = \tau_0 + k\dot{\gamma}^n$$

Where τ is the shear stress, τ_0 is the yield stress, $\dot{\gamma}$ is the shear rate, K is the consistency index (plastic viscosity), k is the flow behaviour index, and n is the flow index.

When these models were fitted to the measured curves, it was found that the Bingham expression was not appropriate to capture the flow relationship; it fails to capture the curvature of the plot, as well as overestimating the yield stress, and was unsuitable at shear rates less than 20 s^{-1}. The Herschel-Bulkley model, in comparison, was more suitable. As the oil loading increased, this model was increasingly notably better at capturing the shear stress-shear rate relationship. Therefore, this implies that at higher wt% oil up to 30%, the material has a more important deviation from a linear (Bingham) relationship.

The Herschel-Bulkley model describes the shear thickening relationship by the n value, Table 4. From 0 to 10 wt% Nevastane loading in the Pickering samples had shear thickening from 1.4 to 0.8 (43 % increase); Table 4. When the Nevastane oil is incorporated into the geopolymer matrix, it forms an immiscible layer with interfacial tension, reducing the geopolymer flowability and increased viscosity. Hence, the successful incorporation of the Nevastane oil in the Pickering samples (excluding the 40 wt% Nevastane oil loading) increased the viscosity of the geopolymer liquid, requiring more force for the material to flow.

Table 4 – The Herschel-Bulkley model parameters calculated for geopolymer cement samples with various weight percentages of Nevastane via the Direct and Pickering methods (1 wt% silica used based on the oil loading). $R^2 \geq 0.99$ for all samples, the Herschel-Bulkley model is able to successfully describe the measured behaviour.

Nevastane wt%	Immobilisation (encapsulation) route	Yield Stress (Pa)	k ($Pa.s^n$)	n
0		6.03	0.16	1.39
10	Direct	9.37	1.53	0.92
20	Direct	26.08	11.19	0.74
30	Direct	15.99	20.06	0.59
40	Direct	2.88	0.93	0.97
10	Pickering	6.04	5.00	0.84
20	Pickering	22.82	11.80	0.74
30	Pickering	20.49	12.36	0.70
40	Pickering	3.66	0.74	1.02

The Pickering samples from 10 to 30 wt% Nevastane have slightly lower yield stress than the non-emulsified Nevastane geopolymer samples, Figure 7, due to the addition of the silica particles. The silica particles create the Pickering emulsion, hence, in theory, reducing the liquid-liquid tension of the Nevastane oil within the geopolymer matrix [13]. The reduced surface tension between the liquids requires less force for the system to flow, hence, the slightly reduced yield stress for the Pickering samples.

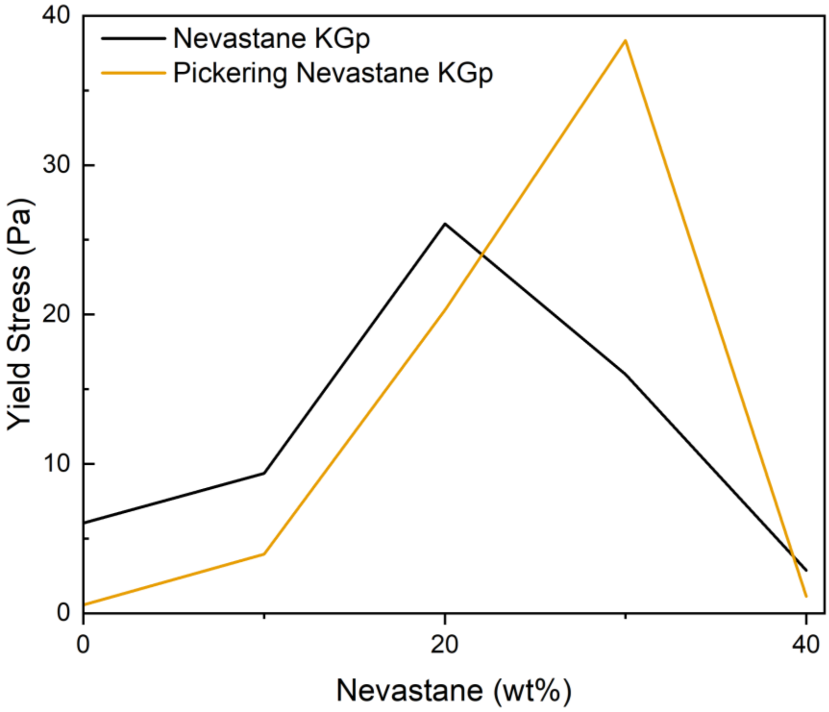

Figure 7 – The yield stress of Pickering and direct immobilisation geopolymer samples increasing weight per cent of Nevastane.

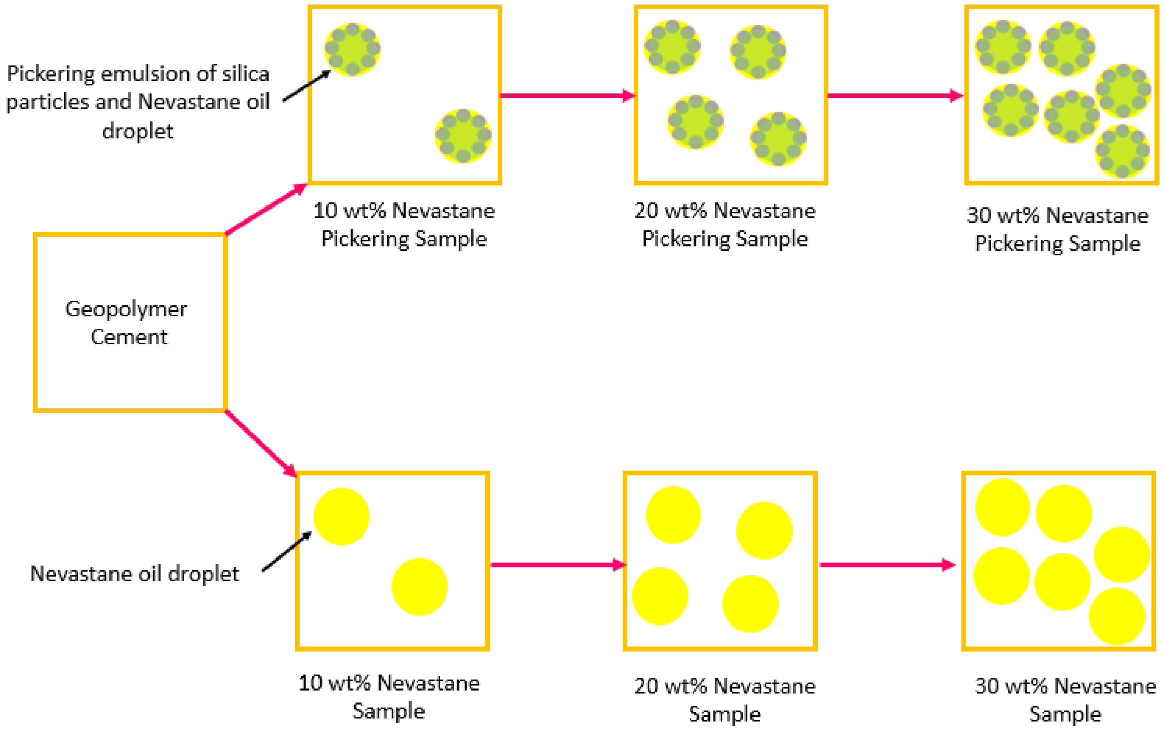

Figure 8 – Schematic sketch of the difference between Pickering and non-Pickering samples with increasing Nevastane loading

3.3 Setting Times

The geopolymer samples containing Pickering emulsions of Nevastane oil with 1 wt% silica particles followed a linear relationship, whereby increasing the oil content increased both the initial and final setting times of the geopolymer matrix, Figure 9. This is because the increasing quantity of organic oil interrupts the formation of the geopolymer, therefore, requiring a longer initial and final setting time [3], [34].

However, it is interesting to note the effect of the silica fume on the setting times in comparison to potassium geopolymer cement with no oil immobilised, Figure 9. For the Pickering cements (with 1 wt% silica particles based on the oil loading) up to 20 wt% Nevastane immobilised the initial and final setting times of these samples are faster than geopolymer cement with no oil immobilised. In the literature, it was found that the addition of silica fume was able to improve mechanical properties such as setting time as the silica fume is an excellent alkali material [20-22]. Therefore, the silica fume can contribute to the formation of the geopolymer cements at low oil loadings, 10 and 20 wt%, to have faster initial and final setting times in comparison to the reference geopolymer sample. At the higher loading of 30 wt%, the high weight percentage of the oil and silica fume likely extended the setting time, in comparison to the reference sample, because the oil is hindering the geopolymer reaction.

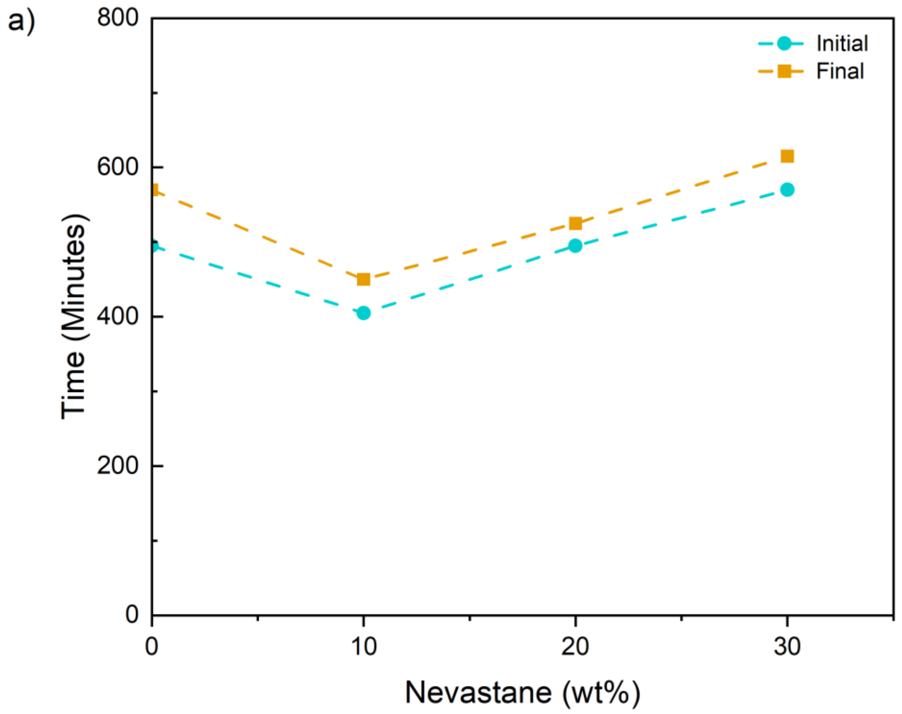
a)
Time (Minutes)
800
600
400
200
0
0
10
20
30
Nevastane (wt%)
Initial
Final

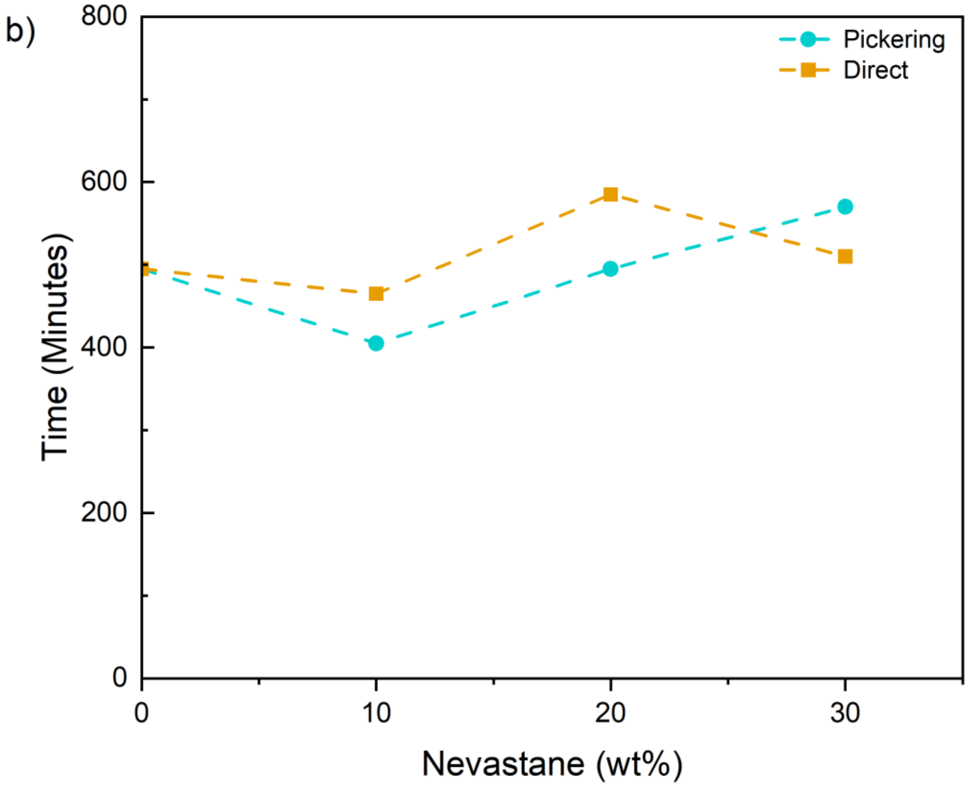
b)
Time (Minutes)
800
600
400
200
0
0
10
20
30
Nevastane (wt%)
Pickering
Direct

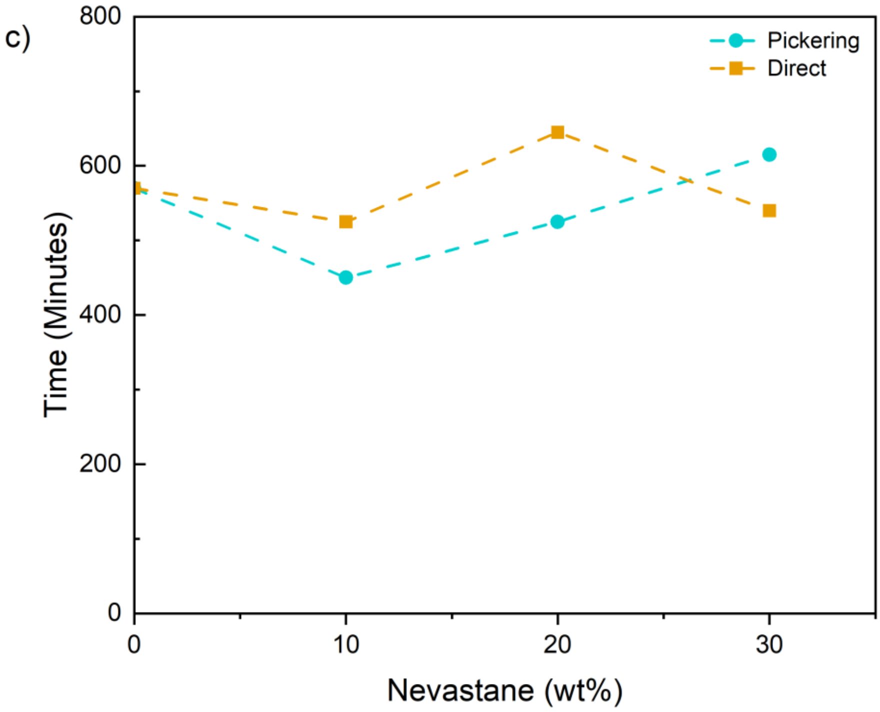

Figure 9 – a) The initial and final setting times of potassium geopolymer cement as a function of the weight percentage of Nevastane, with silica fume being used to create a Pickering emulsion b) The initial setting times of potassium aluminosilicate geopolymer cement with and without the Pickering emulsion, as a function of the loading of Nevastane c) The final setting times of potassium aluminosilicate geopolymer cement with and without the Pickering emulsion, as a function of the loading of Nevastane

When the setting times of the Pickering emulsion geopolymer samples were compared to samples with non-emulsified oil, it was found that samples from 10 to 20 wt% Nevastane were quicker to set with the Pickering emulsion samples; Figure 9. This faster setting time is due to the effect of creating the Pickering emulsion as it reduces the retardation effect that the incorporation of the Nevastane has on the geopolymer gel formation, hence giving a quicker setting time. The 30 wt% Pickering sample was slower to set than the non-emulsified 30 wt% Nevastane sample. However, the non-emulsified 30 wt% Nevastane sample was found to have notable liquid separation so the setting times are not representative of 30 wt% Nevastane actually being incorporated into the geopolymer microstructure. Conversely, the 30 wt% Pickering sample did not have liquid separation and was successful in immobilising this loading of Nevastane oil. It should be noted that the 10 wt% Nevastane geopolymer with direct immobilisation had slightly faster initial and final setting times than the potassium geopolymer cement. This is believed due to systematic error in either the preparation or running of the potassium geopolymer sample without oil, as the direct immobilisation samples follow a linear trend as the oil wt% increases. Furthermore, all the samples do not fall within the industry standards (ATSM C191) of an initial setting time of 30 to 120 minutes and a final set within 6.5 hours [27]. However, ATSM C191 is a standard for hydraulic cement, particularly intended for Portland cement in construction applications and therefore requiring a faster initial and final setting time than is particularly necessary for wasteform cements [27, 35]. Therefore, this standard required setting time should be used more as a suggestion than a strict rule to account for the different type of cement used in this work as well as the addition of the organic oil.

In conclusion, the formation of a Pickering emulsion with 1 wt% silica particles for incorporating 10 and 20 wt% of Nevastane oil had faster setting times than geopolymer with no oil, and their non-emulsified equivalents. This was believed to be due to the silica particles acting as an alkali-reactive material, increasing the rate of geopolymer gel formation which reduced setting times. [20-22]. Furthermore, the silica particles could form a Pickering emulsion with the Nevastane oil, reducing the surface contact of the oil so it does not hinder the geopolymer formation.

3.4 Compressive Strength

The effect of adding 1 wt% silica particles to create a Pickering emulsion to further aid in the immobilisation of Nevastane at different weight percentages at seven days is shown in Figure 10. At seven days, the compressive strength is significantly higher for the 10 wt% Pickering sample compared the non-emulsified 10 wt% Nevastane sample. The 20 wt% Nevastane Pickering samples also have slightly higher compressive strengths than their non-emulsified counterparts; Figure 10. This shows the beneficial effect of adding silica particles, especially in aiding with structural strength in the early setting of the samples which is consistent with the setting times found in Section 3.3. Furthermore, the addition of the organic oil increases the setting time of the geopolymer cement as it interrupts the geopolymerisation reaction. The formation of a Pickering emulsion can disperse the Nevastane droplets throughout the geopolymer matrix, hence, reducing the negative effect of the oil on the geopolymer formation, so more of the gel is allowed to form within seven days.

However, the 30 wt% Pickering Nevastane sample had a decreased compressive strength compared to the non-emulsified 30 wt% Nevastane sample at seven days. The reason for this could potentially be due to the increasing mass of silica fume being incorporated in the geopolymer matrix. The amount of silica fume added to the geopolymer system is based on 1 wt% of the oil. Therefore, with increasing oil loadings there is more silica fume in the system. Zawrah *et al.* [22] also found that there was an optimism silica incorporation of 2.5 %. Above 2.5 % nano-silica, the compressive strength decreased due to the nano-SiO_2 particles aiding in the breakdown of the geopolymer gel. This would make sense as the weight percentage of the silica fume is added based on the weight of the oil. Therefore, as the oil loading increases, more silica fume is being added to the geopolymer system with decreased metakaolin and alkali activating solution. Conversely, it is also possible that the separation of the oil out from the non-emulsified 30 wt.% samples may have left a lower effective oil loading – and therefore a higher strength – in the remaining part of the geopolymer sample, even though the immobilisation was not effective in this instance.

After 28 days of curing, the Pickering samples were again tested for their compressive strength. All of the Pickering samples had a decrease in their compressive strength compared to their non-emulsified counterparts, Figure 10. Svinstov & Shambina [36] found that mineral oils incorporated into hardened cement (cured for 28 days before adding oil) filled the cement pores as a hydraulic material and behaved like an incompressible fluid, reducing their compressive strength. Furthermore, Ahmed *et al.* [37] concluded that alongside filling pores, the unreacted nano-silica was able to accelerate the geopolymer reaction since it is rich in silica. Hence, any nano-silica that was not in the Pickering emulsion would be able to aid in the acceleration of the geopolymerisation reaction. This explains why the Pickering samples have early age strength as it is rapidly forming the geopolymer chains but the strength decreases at 28 days as the geopolymer chains are not of good quality/poor interconnect of the chains [38]. Even with the decrease, all of the Pickering samples were above the UK industry minimum waste form strength of 7 MPa, so are potentially acceptable in terms of this performance criterion [39].

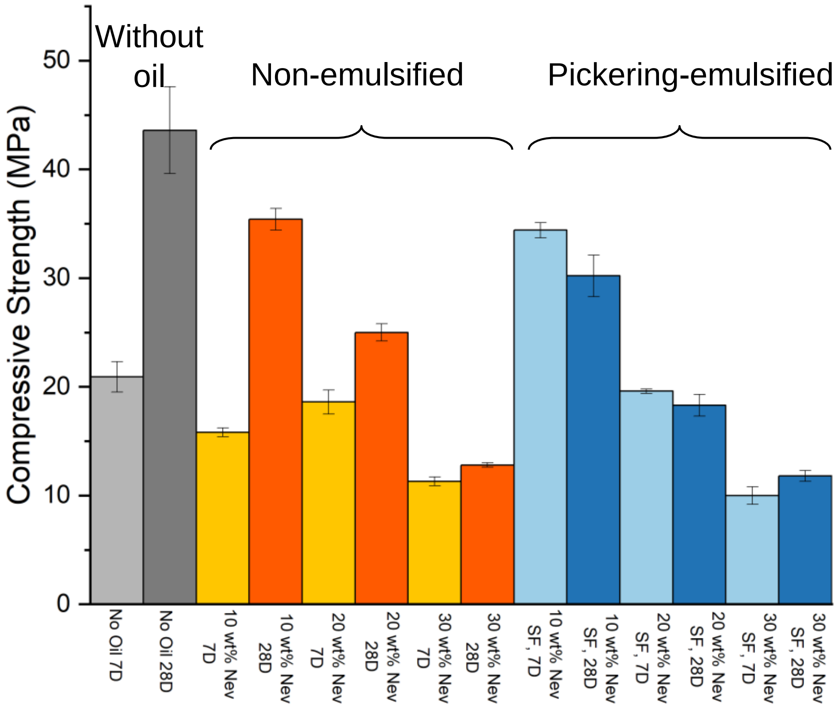

Figure 10 – The compressive strengths of potassium geopolymer cements with no oil, 10 – 30 wt% non-emulsified Nevastane, and 10 – 30 wt% Pickering Nevastane emulsion, at 7 (lighter shaded columns) and 28 (darker shaded columns) days.

3.5 FTIR

The FTIR spectra measured for both Nevastane and TBP/dodecane oil-containing geopolymer samples contained peaks indicative of the formation of the geopolymer, Figure 11. These included a medium peak because of symmetrical stretching at 620 cm^{-1} of Si-O-Si and Al-O-Si [40]. A medium peak at 720 cm^{-1} is due to pseudolattice vibrations of small aluminosilicate rings [40]. An intense peak is between 900 – 1000 cm^{-1} because of non-bridging oxygen in the Si-O bond and the asymmetric stretching of Si-O-(Al, Si) [40]. This peak shows that a (N, K)-A-S-H gel has been formed in the geopolymer structure. Asymmetric stretching of Al-O-Si at 870 cm^{-1} as a medium peak shows the linking of the AlO_4 and SiO_4 groups [40]. A small peak at 1600 cm^{-1} due to chemically bound and free water. A small peak at 2341 cm^{-1} is due to atmospheric carbon dioxide. A broad peak from 3000 – 3200 cm^{-1} is due to O-H stretching in the pore water [40]. This highlights that the geopolymer gel has been successfully formed at seven days (Section 3.3) and the addition of either oil did not negatively affect this process.

For the geopolymers with various weight percentages of TBP/dodecane, there was a small peak at 2950 cm^{-1} which relates to the C-H stretching of the alkane. There were also small peaks at 1365 and 1469 cm^{-1} due to C-H bending [40]. These peaks suggest the presence of an alkane in the geopolymer system. The FTIR spectra of TBP and dodecane showed peaks at 1300 – 1400 and 2950 cm^{-1} relating to the bending and stretching of the C-H bonds, Figure 11, confirming that the alkane peaks in the Pickering samples belong to the oil. There are no additional peaks in the FTIR spectra that are not either due to the geopolymer gel or the organic oil. This suggests that the oil did not chemically interact with the alkaline environment of the geopolymer matrix. Furthermore, the small peaks at 1300 – 1500 and 2950 cm^{-1} only increased slightly with the increasing wt% of the TBP/dodecane being added to the geopolymer system. This was because the liquid-liquid separation of the TBP/dodecane increased as the wt% loading increased. The maximum wt% that the geopolymer could contain was reached before the 10 wt% loading. This relates to how the samples formed when they were made. For the TBP/dodecane sample, A1, a layer of liquid had to be removed before the sample could be prepared for analysis. Therefore, it did not matter if the wt% loading of the TBP/dodecane was increased from 10 to 40 wt%, the geopolymer matrix was unable to incorporate any more TBP/dodecane as it had already reached its maximum weight loading. This suggests that the Pickering emulsion route was not suitable for aiding the incorporation of TBP/dodecane even at low loadings. It is difficult to allow for direct quantification of the immobilised TBP/dodecane as it requires successful immobilisation of the TBP/dodecane to create a calibration curve from the FTIR spectra, and this has not yet been possible.

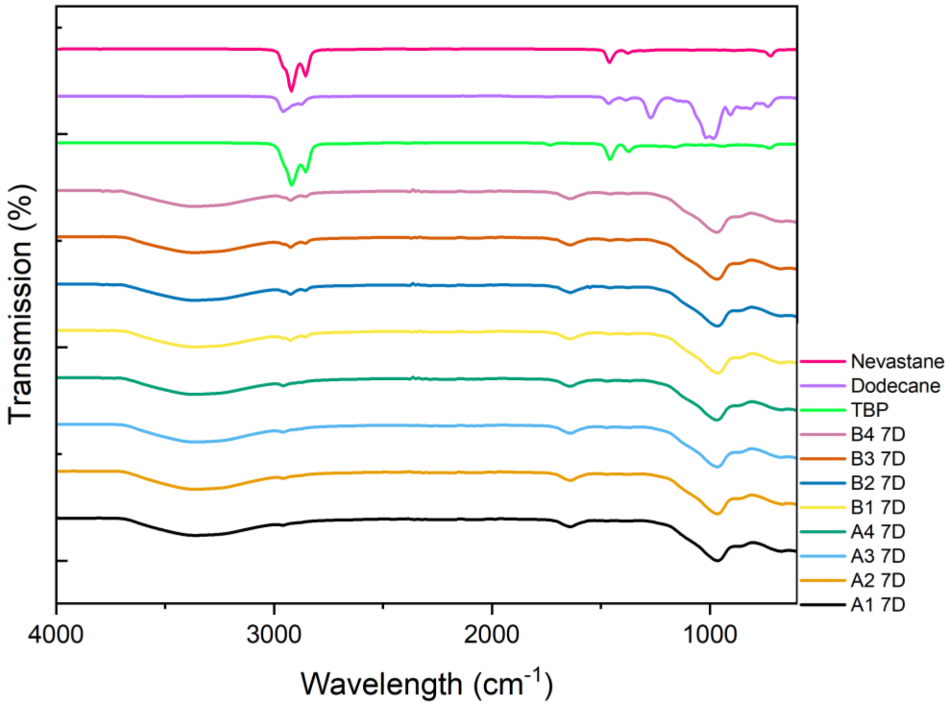

Figure 11 – Offset plot of FTIR spectra of Samples A1, A2, A3, A4, B1, B2, B3 and B4 after seven days of curing, as well as TBP, dodecane and Nevastane oil

For the geopolymers with various weight percentages of Nevastane, there was a double peak between 1300 – 1500 cm^{-1} and a peak with a shoulder at 2950 cm^{-1}, Figures 11 and 12 These peaks were due to the C-H bending and stretching of alkanes in the Nevastane oil; Figure 11. The peak is distinct and is similar in intensity for the increasing wt% of the Nevastane incorporated.

This can be related to the observed results when making the geopolymer samples for Nevastane incorporation. When the B1–4 samples were mixed, samples B1-3 (up to 30 wt.% loading) had no signs of liquid separation, and the Nevastane oil was successfully incorporated into the geopolymer matrix. Hence, the increased peaks at 1300 - 1500 and 2950 cm^{-1} for B1 to B3 are due to a higher incorporation of Nevastane oil into the geopolymer matrix. However, when B4 was mixed it had a 'shiny' surface and began to show oil separation from the geopolymer matrix. This is why B4 has lower peaks at 1300 - 1500 and 2950 cm^{-1} as there was less oil in the geopolymer matrix; Figure 12. The oil loading had reached the critical limit above 30 wt% Nevastane loading for the geopolymer matrix, and it was more favourable for the oil to coalesce and separate from the geopolymer matrix. These trends followed the physical observations noted during the mixing of B1 – 4, where 10 – 30 wt% Nevastane mixed with no signs of oil separation, while the 40 wt% Nevastane sample had a ‘shiny’ surface due to the start of oil separation. Hence, it can be concluded that the Pickering emulsion was successful in aiding the incorporation of ≤ 30 wt% Nevastane oil into the geopolymer matrix.

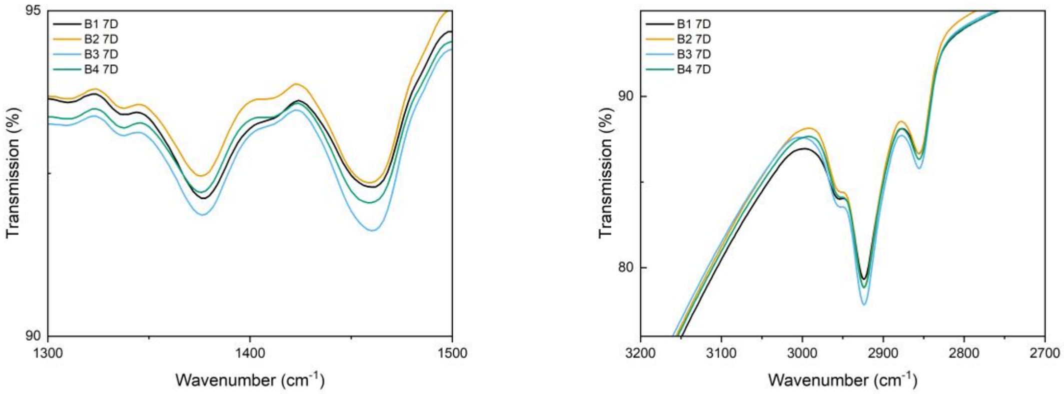

Figure 12 – The FTIR spectra of Samples B1–4 enlarged to show the trend in the C-H bending and stretching due to the incorporation of Nevastane oil, highlighting the peaks at 1300 – 1500 and 2950 cm^{-1}

3.6 XRD

XRD data were collected for samples A1–4 and B1–4 after 90 days of curing, and the diffractograms all showed an amorphous hump with minor peaks due to anatase (TiO_2); Figure 13. The silica particles did not appear to form any crystalline phases within the geopolymer matrix. When compared to the Metamax metakaolin and silica particle precursors, the source of the anatase appears to have been the impurities in the metakaolin precursor; Figure 13. In the XRD diffractograms of the silica particles, there is a peak at 35° 2θ due to the presence of quartz [41], that was not found in the Pickering samples, maybe due to the rather low content of silica fume added to each of these samples. However, the residual silica fume particles are seen clearly by a broad feature in the diffractograms at 35° 2θ, indicating that at least a significant fraction of the silica fume particles remained intact within the Pickering-emulsified particles and did not participate in the geopolymer formation reactions despite the very high pH conditions within these samples.

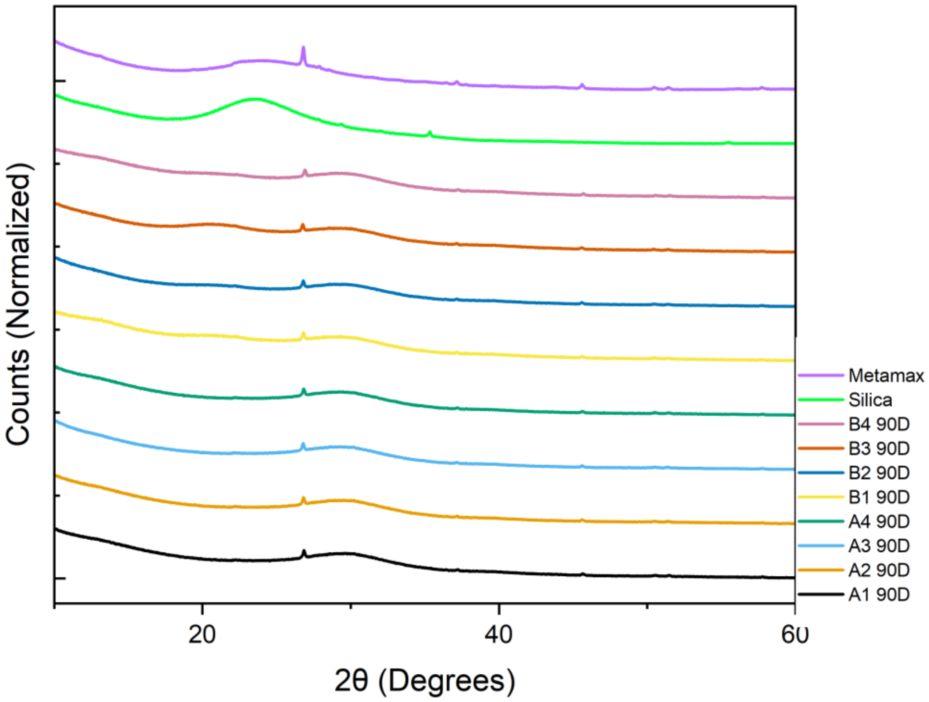

Figure 13 – Offset XRD diffractograms for the Pickering emulsion samples with various wt% of Nevastane and TBP/dodecane, after 90 days of curing as well as Silica and Metamax metakaolin

3.7 X-Ray Tomography

The X-ray tomography reconstructions showed that the Nevastane oil was distributed throughout the geopolymer matrices as spherical droplets; Figure 14. As the oil incorporation increased, the Pickering emulsion was shown to prevent the coalescence of the droplets up to a higher Nevastane loading, which is consistent with the zeta potential data in Section 3.1.

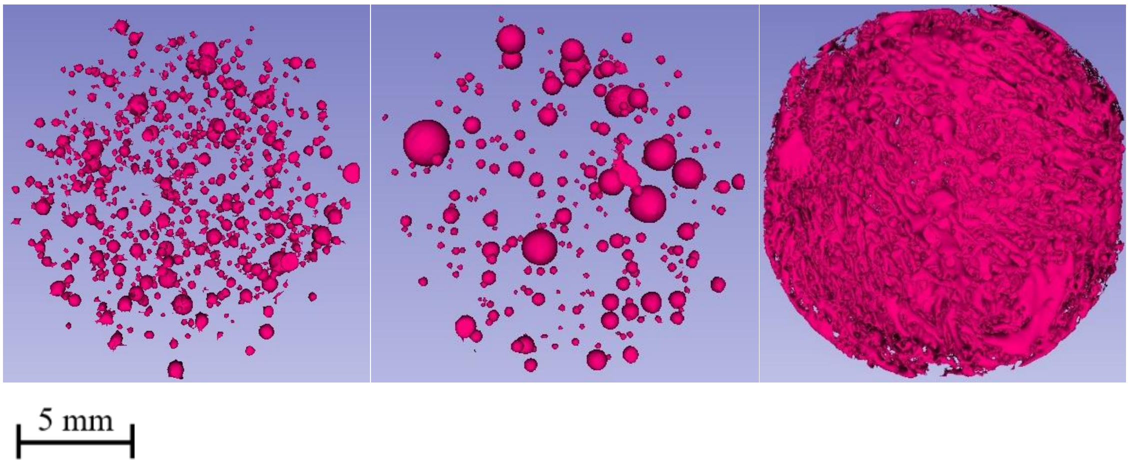

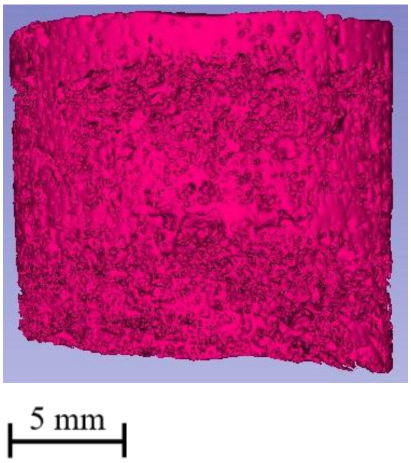

Figure 14 - The 3D constructed images via 3D Slicer for 10, 20, 30 and 40 wt% Nevastane Pickering samples, from left to right, respectively. The field of view used was 1024 pixels at 15 μm/pixel, to give a field size of 15.36 mm.

When the Pickering Nevastane samples were compared to the non-emulsified Nevastane samples, the total area of the oil droplets was similar for both, when loaded with up to 20 wt% of Nevastane oil, Figure 15. However, at 30 wt% Nevastane, the Pickering geopolymer samples had a higher total area of oil distributed throughout the sample than the 30 wt% non-emulsified Nevastane sample; Figure 20 shows the data separated into quantifications of regions of interest located at the top, middle, and bottom of each sample to enable the homogeneity of oil distribution to be assessed. These results suggest that the Pickering-emulsified sample could incorporate a higher content of oil before droplet coalescence occurs. Furthermore, even though both the 40 wt% Pickering and non-emulsified Nevastane samples underwent oil separation, determination of the total area from these tomography data shows that the non-emulsified sample had a higher area at the top of the sample compared to the Pickering sample; Figure 15. This suggests that the non-emulsified sample underwent higher oil separation than the 40 wt% Pickering sample.

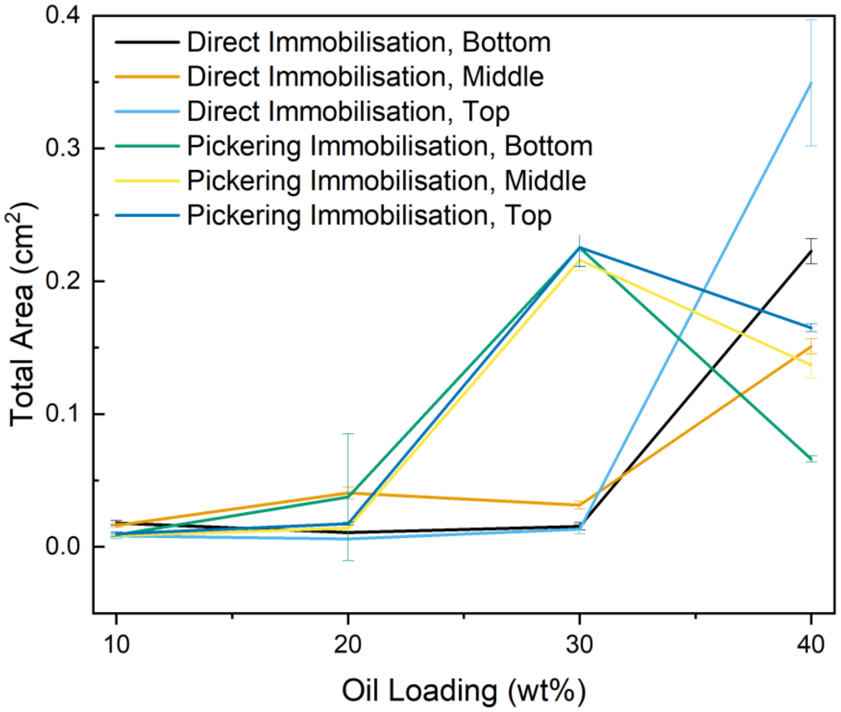

Figure 15 – The total area of the oil droplets through the cement samples for 10 – 40 wt% Nevastane non-emulsified and Pickering emulsion, where the bottom, middle and top annotations refer to the section of the sample where to the total area of the oil droplet was measured.

4. Conclusions

In this study, the use of Pickering emulsion was investigated as a route to immobilise liquid organic oil by creating an emulsification before mixing it into the cement slurry. Upon physical observation of the samples being mixed, there was a clear difference between the behaviour of the organic oils. Nevastane was readily immobilised by the Pickering emulsion technique up to 30 wt% loading in the geopolymer; beyond this level, there was liquid separation. However, TBP/dodecane did not successfully immobilise at any of the loadings tested, suggesting that the Pickering emulsion approach was not enough to aid in the immobilisation of this particular organic liquid.

The zeta potential measurements showed that the silica particles have a negative surface charge, similar to the metakaolin precursor. The negative charge on the silica particles is able to aid in dispersing the Nevastane oil in the geopolymer matrix. This avoids oil coalescence via the Pickering emulsion, hence, reducing the likelihood for oil separation from the geopolymer matrix. The rheology of the Nevastane samples showed increased shear thickening as the oil loading increased with a maximum of 30 wt%.

The Pickering emulsion geopolymer samples had quicker initial and final setting when compared to the non-emulsified Nevastane oil-containing samples, except for the case of the 30 wt% loading. The Pickering emulsion reduced surface contact of the Nevastane oil so the geopolymer gel was able to form quicker. Furthermore, the silica particles could also have acted in part as alkali-reactive material which helped speed up the formation of the geopolymer gel, although the X-ray diffraction analysis showed the presence of remnant silica and indicted that they could not have been fully consumed through this type of process.

All of the Pickering samples had higher early compressive strength than the non-emulsified Nevastane sample after 7 days. This was believed to be due to both the lower surface contact of the Nevastane oil that did not hinder the formation of the geopolymer gel, and the alkali-reactive behaviour of the silica particles which helped increase the rate of geopolymerisation. After 28 days, all the Pickering samples had lower compressive strengths compared to their non-emulsified counterparts, but were still above the UK industry minimum of 7 MPa, indicating the potential for acceptability in practice. X-ray tomography showed that the Pickering emulsion was successfully in dispersing the Nevastane droplets throughout the geopolymer matrix, with good uniformity of the droplet distribution up to 30 wt% loading.

5.0 Acknowledgements

The authors acknowledge the financial support of PREDIS (the PREDIS project has received funding from the Euratom research and training programme 2019-2020 under grant agreement No 945098) and the EPSRC GREEN CDT (EP/S022295/1), and the constant support of the Cements@Sheffield and SMASH research groups. We thank the PREDIS WP5 partners, particularly Martin Hayes of NNL, for discussions and ongoing collaboration related to geopolymer mix design development and validation in the context of radioactive waste immobilisation.

6.0 References

1. Hyatt, N.C. and M.I. Ojovan, *Materials for nuclear waste immobilization*. Materials, 2019, 12(21), #3611.
2. Tsang, D. and L. Wang, *Low Carbon Stabilization and Solidification of Hazardous Wastes*. 2022: Elsevier.
3. Reeb, C., et al., *Incorporation of organic liquids into geopolymer materials-A review of processing, properties and applications.* Ceramics International, 2021. **47**(6): p. 7369-7385.

4. Drinks, E., et al., *UV-a photocatalytic degradation of the radionuclide complexants tributylphosphate and dibutylphosphate.* Chemical Engineering Journal, 2018. **352**: p. 143-150.

5. Reeb, C., et al., *Incorporation of organic liquids into geopolymer materials - A review of processing, properties and applications.* Ceramics International, 2021. **47**(6): p. 7369-7385.

6. Lambertin, D., A. Rooses, and F. Frizon, *Process for preparing a composite material from an organic liquid and resulting material*. 2019, US Patent 10,450,231B2

7. Pierlot, C., et al., *Selection of suitable surfactants for the incorporation of organic liquids into fresh geopolymer pastes.* Chemical Engineering Science, 2022. **255**: #117635.

8. Cantarel, V., et al., *Geopolymer assembly by emulsion templating: emulsion stability and hardening mechanisms.* Ceramics International, 2018. **44**(9): p. 10558-10568.

9. Pickering, S.U., *CXCVI. - emulsions.* Journal of the Chemical Society, Transactions, 1907. **91**: p. 2001-2021.

10. Bertin, M., et al., *Influence of cetyltrimethylammonium bromide and hydroxide ions on the interfacial tension and stability of emulsions of dodecane in aqueous silicate solutions.* Colloids and Surfaces A: Physicochemical and Engineering Aspects, 2021. **628**: #127306.

11. El-Naggar, M.R., E.A. El-Sherief, and H.S. Mekhemar, *Performance of geopolymers for direct immobilization of solvent extraction liquids: Metakaolin/LIX-84 formulations.* Journal of Hazardous Materials, 2018. **360**: p. 670-680.

12. Mossini, E., et al., *Pre-impregnation approach to encapsulate radioactive liquid organic waste in geopolymer.* Journal of Nuclear Materials, 2023. **585**: #154608.

13. de Carvalho-Guimarães, F.B., et al., *A review of Pickering emulsions: Perspectives and applications.* Pharmaceuticals, 2022. **15**(11): #1413.

14. Yuan, C., et al., *Study on characteristics and harm of surfactants.* Journal of Chemical and Pharmaceutical Research, 2014. **6**(7): p. 2233-2237.

15. Yang, Y., et al., *An overview of Pickering emulsions: solid-particle materials, classification, morphology, and applications.* Frontiers in Pharmacology, 2017. **8**: #287.

16. Chu, S. and A. Kwan, *Co-addition of metakaolin and silica fume in mortar: Effects and advantages.* Construction and Building Materials, 2019. **197**: p. 716-724.

17. Levine, S., B.D. Bowen, and S.J. Partridge, *Stabilization of emulsions by fine particles I. Partitioning of particles between continuous phase and oil/water interface.* Colloids and Surfaces, 1989. **38**(2): p. 325-343.

18. Griffith, C. and H. Daigle, *Destabilizing Pickering emulsions using fumed silica particles with different wettabilities.* Journal of Colloid and Interface Science, 2019. **547**: p. 117-126.

19. Frelichowska, J., M.-A. Bolzinger, and Y. Chevalier, *Pickering emulsions with bare silica.* Colloids and Surfaces A: Physicochemical and Engineering Aspects, 2009. **343**(1-3): p. 70-74.

20. Zhang, P., et al., *Effect of single and synergistic reinforcement of PVA fiber and nano-SiO_2 on workability and compressive strength of geopolymer composites.* Polymers, 2022. **14**(18): #3765.

21. Lo, K.-W., et al., *Effect of nano-SiO_2 on the alkali-activated characteristics of spent catalyst metakaolin-based geopolymers.* Construction and Building Materials, 2017. **143**: p. 455-463.

22. Zawrah, M., et al., *Effect of nano sand on the properties of metakaolin-based geopolymer: Study on its low rate sintering.* Construction and Building Materials, 2020. **246**: #118486.

23. Pancotti, F., et al. *Investigation, Development and Assessment of Innovative Direct Conditioning Solutions for Radioactive Liquid Organic Waste Within the PREDIS Project*. in *International Conference on Radioactive Waste Management and Environmental Remediation*. 2023. American Society of Mechanical Engineers.

24. Geddes, D., *A Study of the Suitability of Metakaolin-based Geopolymers for the Immobilisation of Problematic Intermediate Level Waste*. 2020, Ph.D. thesis, University of Sheffield.

25. ASTM International, *ASTM C150/C150M-21 Standard Specification for Portland Cement*. 2021: West Conshohocken PA.

26. BSI, *BS EN 196-3:2016 Methods of testing cement - Determination of setting times and soundness*. 2016, British Standards Institute: London.

27. Bhatty, J.I. and P.D. Tennis, *US and Canadian cement characteristics: 2004*. 2008: Portland Cement Association Skokie, IL, USA.

28. Abràmoff, M.D., P.J. Magalhães, and S.J. Ram, *Image processing with ImageJ.* Biophotonics International, 2004. **11**(7): p. 36-42.

29. Derkani, M.H., et al., *Mechanisms of dispersion of metakaolin particles via adsorption of sodium naphthalene sulfonate formaldehyde polymer.* Journal of Colloid and Interface Science, 2022. **628**: p. 745-757.

30. Hiemstra, T., J.M. De Wit, and W. Van Riemsdijk, *Multisite proton adsorption at the soil/solution interface of (hydr)oxides: A new approach. II: Application to various important (Hydr) oxides.* Journal of Colloid and Interface Science, 1989. **133**(1): p. 105-117.

31. Behrens, S., M. Borkovec, and M. Semmler, *Aggregation in sulfate latex suspensions: the role of charge for stability predictions.* Trends in Colloid and Interface Science XII, 1998: p. 66-69.

32. Sjöberg, S., *Silica in aqueous environments.* Journal of Non-Crystalline Solids, 1996. **196**: p. 51-57.

33. Low, L.E., et al., *Recent advances of characterization techniques for the formation, physical properties and stability of Pickering emulsion.* Advances in Colloid and Interface Science, 2020. **277**: #102117.

34. A. Hasnaoui, J.M., C. Reeb, M. Hayes, C.A. Davy, J. L. Provis, D. Lambertin, *Solidification of tributyl phosphate/dodecane waste using metakaolin-based potassium geopolymers.* Nuclear Engineering and Design, 2025 (under review).

35. Artanti, L.D., et al. *Comparative study of the use of Ordinary Portland Cement (OPC), Portland Composite Cement (PCC) and Hydraulic Cement (HC) types in high quality concrete with an independent compaction system*. in *E3S Web of Conferences*. 2024. EDP Sciences.

36. Svintsov, A.P. and S.L. Shambina, *Influence of viscosity of vegetable and mineral oil on deformation properties of concrete and cement-sand mortar.* Construction and Building Materials, 2018. **190**: p. 964-974.

37. Ahmed, H.U., et al., *Compressive strength of geopolymer concrete modified with nano-silica: Experimental and modeling investigations.* Case Studies in Construction Materials, 2022. **16**: # e01036.

38. Castillo, H., et al., *Factors affecting the compressive strength of geopolymers: A review.* Minerals, 2021. **11**(12): #1317.

39. Byeon, H., G.Y. Jeong, and J. Park, *Structural stability analysis of waste packages containing low-and intermediate-level radioactive waste in a silo-type repository.* Nuclear Engineering and Technology, 2021. **53**(5): p. 1524-1533.

40. Chukanov, N.V., *Infrared Spectra of Mineral Species: Extended Library*. 2013: Springer Science & Business Media.

41. Villar-Cociña, E., et al., *A comparative study on the pozzolanic activity between bamboo leaves ash and silica fume: Kinetic parameters.* Waste and Biomass Valorization, 2020. **11**: p. 1627-1634.